# Fluorescent multi-component polymer sensors for sensitive and selective detection of $Hg^{2+}$/$Hg^{+}$ ions via fluorescence and colorimetry dual mode

Kaiqi Liu[a], Luminita Marin[b], Li Xiao[a], and Xinjian Cheng[a*]

[a]School of Chemistry and Environmental Engineering, Wuhan Institute of Technology, Wuhan, China, 430073

[b]"Petru Poni'' Institute of Macromolecular Chemistry of Romanian Academy, Iasi, Romania

*Corresponding author: Dr. Cheng, chxj606@163.com.

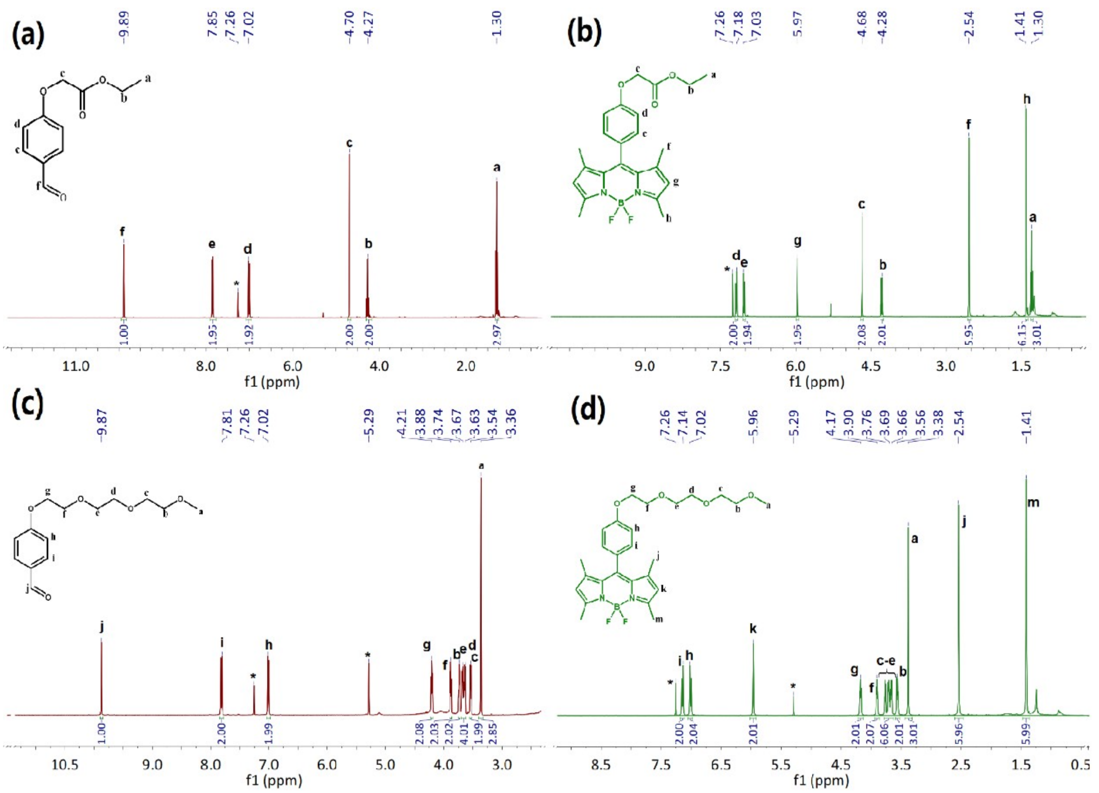


**Figure S1.** $^1$H NMR spectra of small molecule compounds (a) **O1**, (b) **BO1**, (c) **O2**, and (d) **BO2**

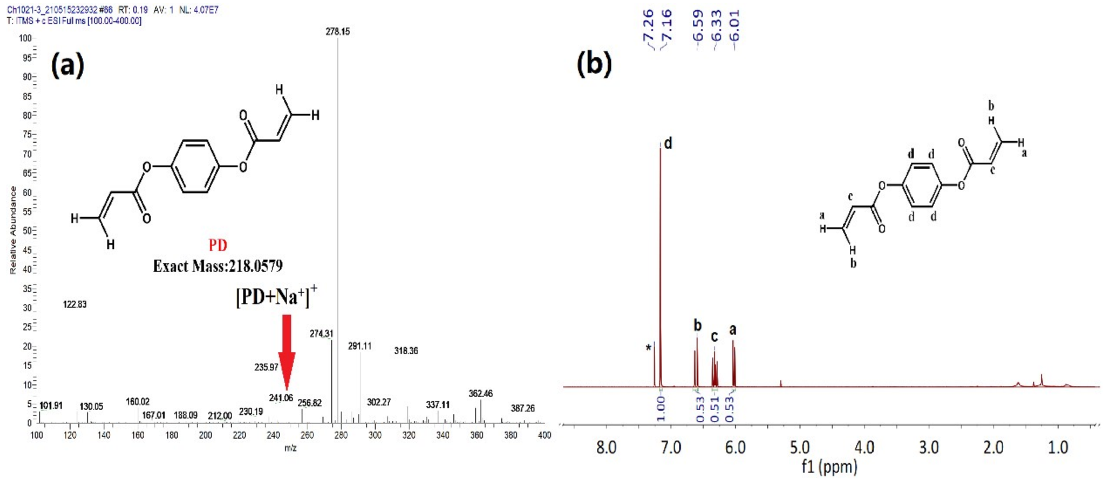


**Figure S2.** (a) $^1$H NMR spectra of small molecule compounds **PD** (b) Mass spectra of **PD**

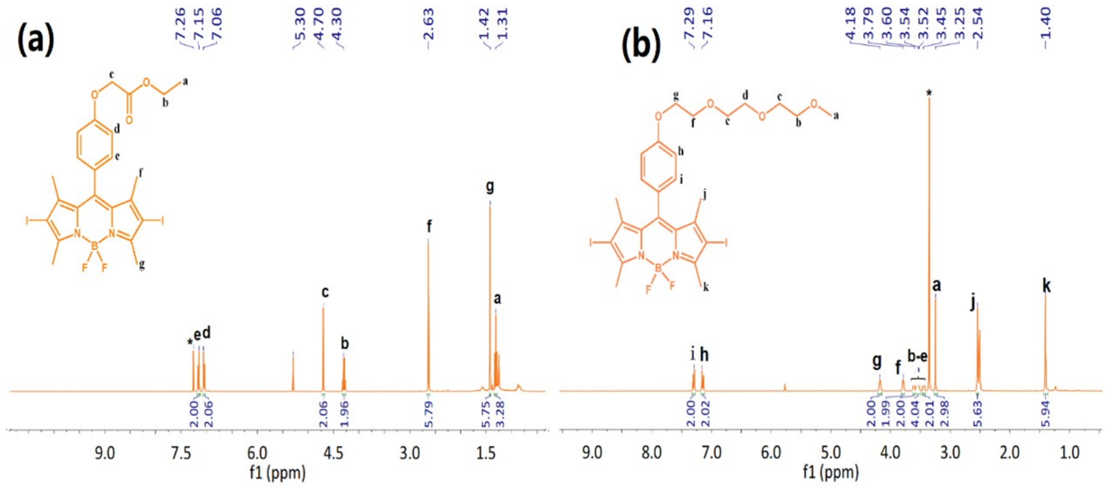


**Figure S3.** $^1$H NMR spectra of small molecule compounds (a) **IBO1** and (b) **IBO2**

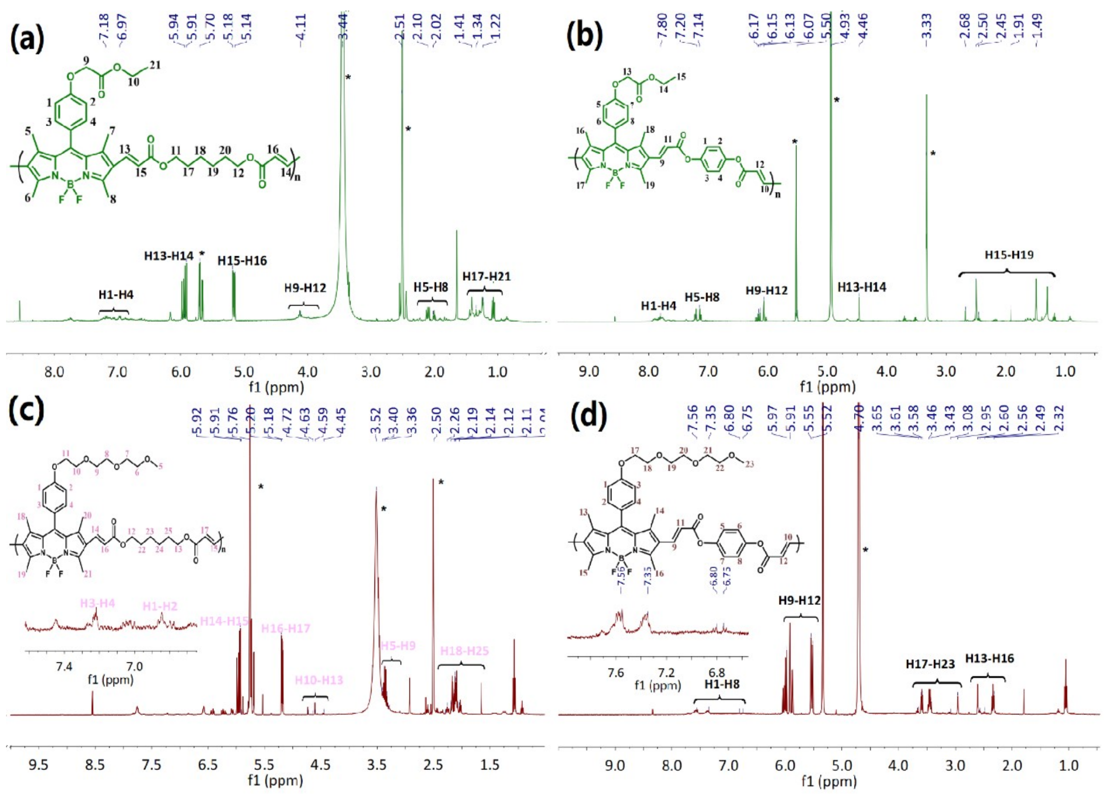


**Figure S4.** $^1$H NMR spectra of polymer probes (a) **MCP1**, (b) **MCP2**, (c) **MCP3**, and (d) **MCP4**

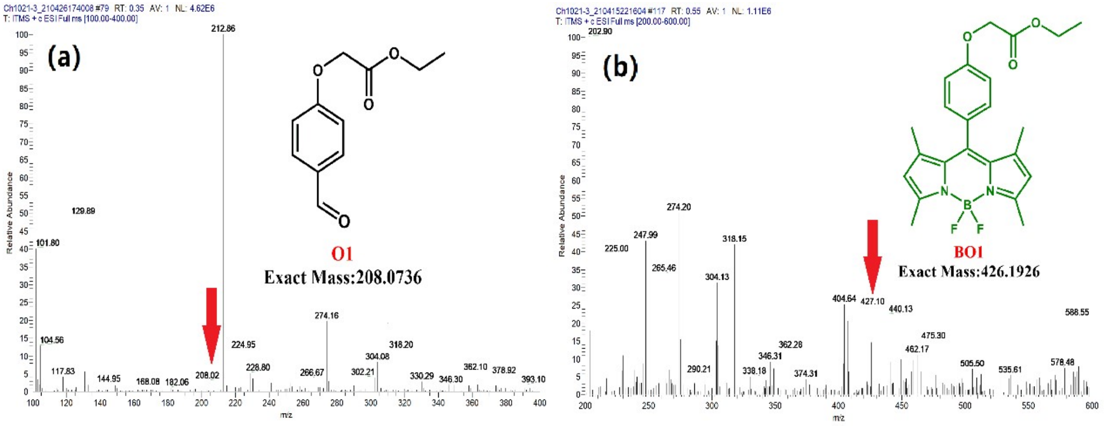


**Figure S5.** ESI-HRMS spectrum of (a) **O1** and (b) **BO1**

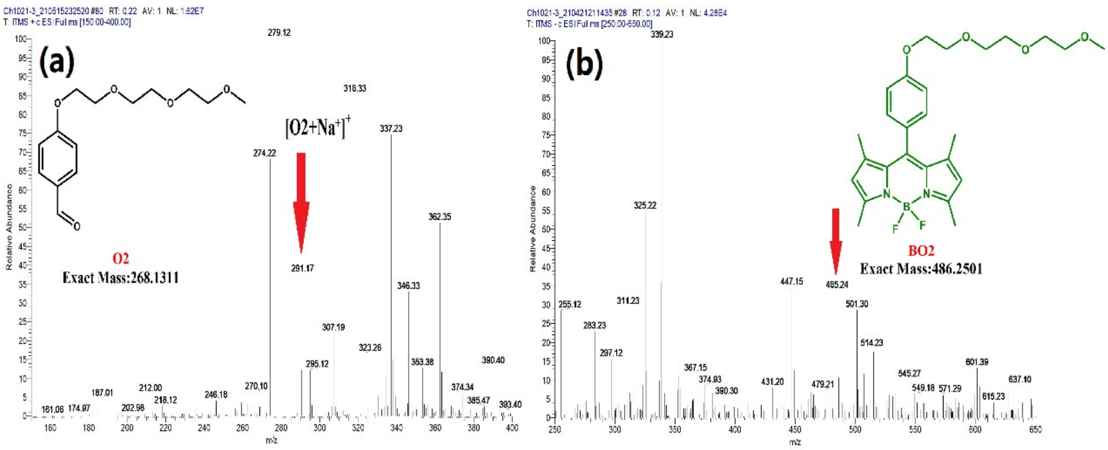


**Figure S6.** ESI-HRMS spectrum of (a) **O2** and (b) **BO2**

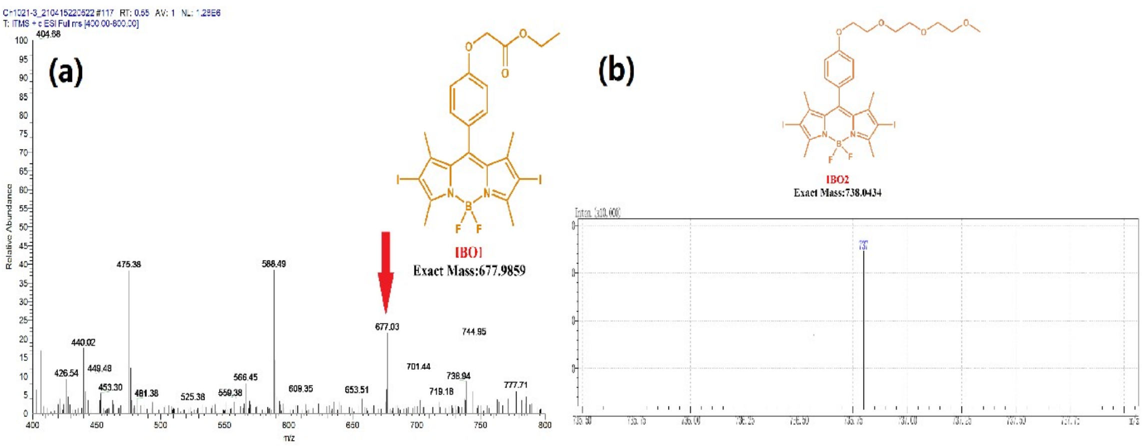


**Figure S7.** ESI-HRMS spectrum of (a) **IBO1** and (b) **IBO2**

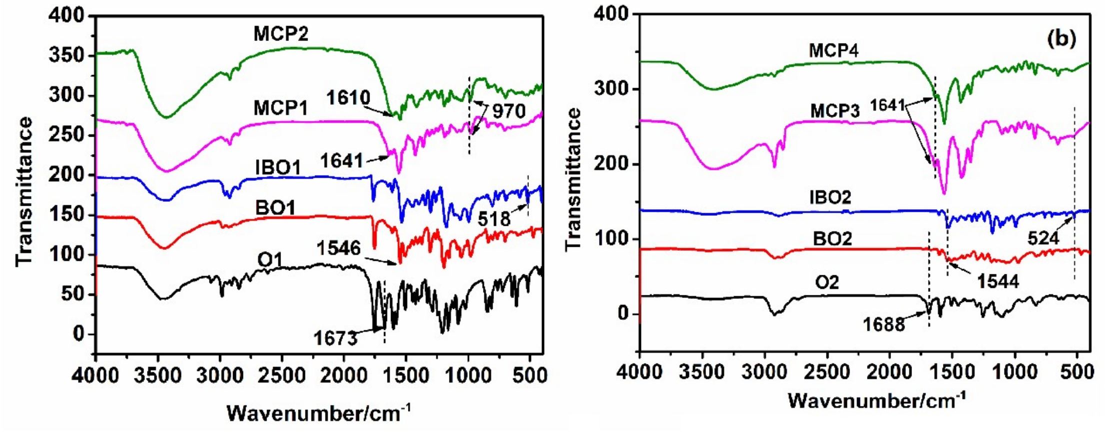


**Figure S8.** FTIR spectra of (a) **O1**, **BO1**, **IBO1**, **MCP1** and **MCP2** and (b) **O2**, **BO2**, **IBO2**, **MCP3** and **MCP4**

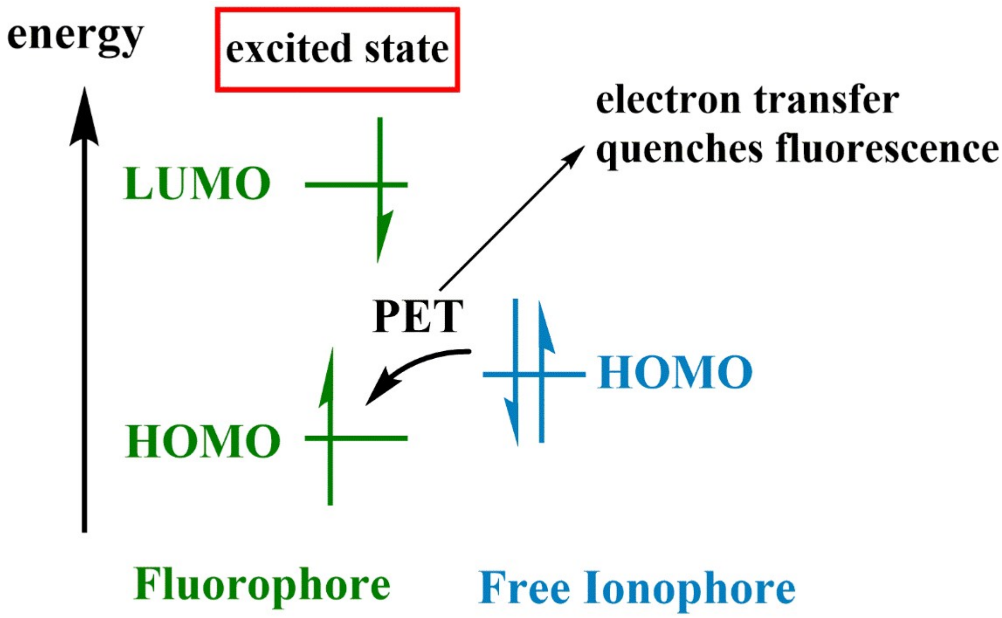


**Figure S9.** The mechanism of PET

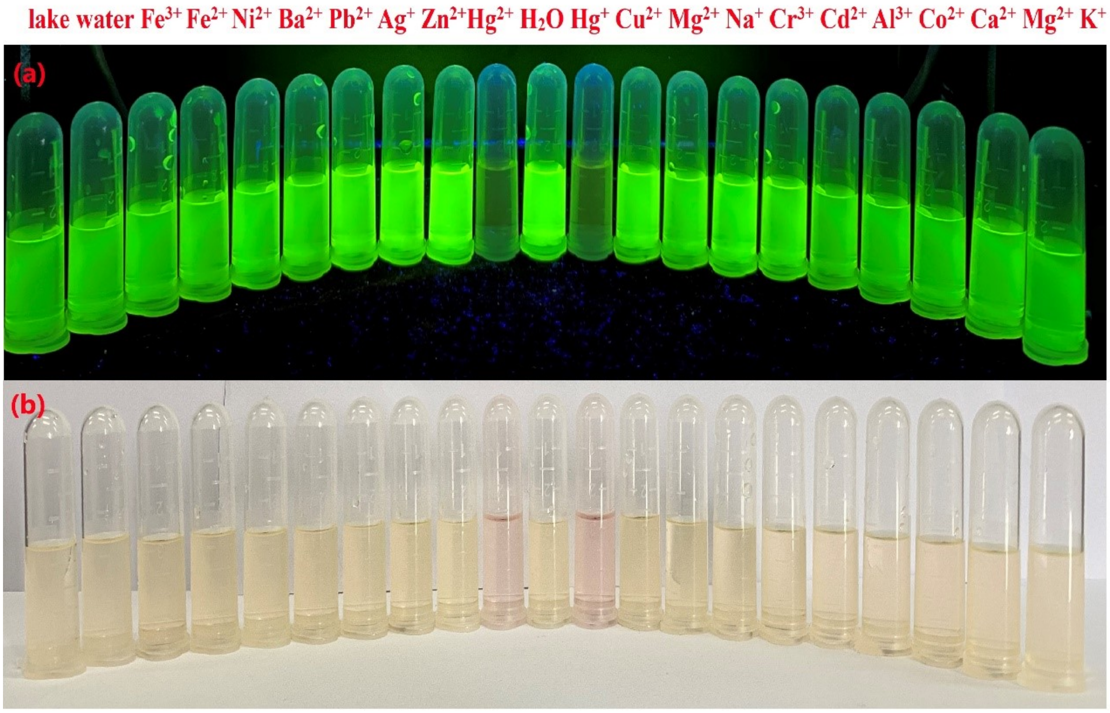


**Figure S10.** (a) photograph of **MCP1** with heavy metal ion in EtOH/$H_2O$ under UV light. (b) photograph of **MCP1** with heavy metal ion in EtOH/$H_2O$ under natural light.

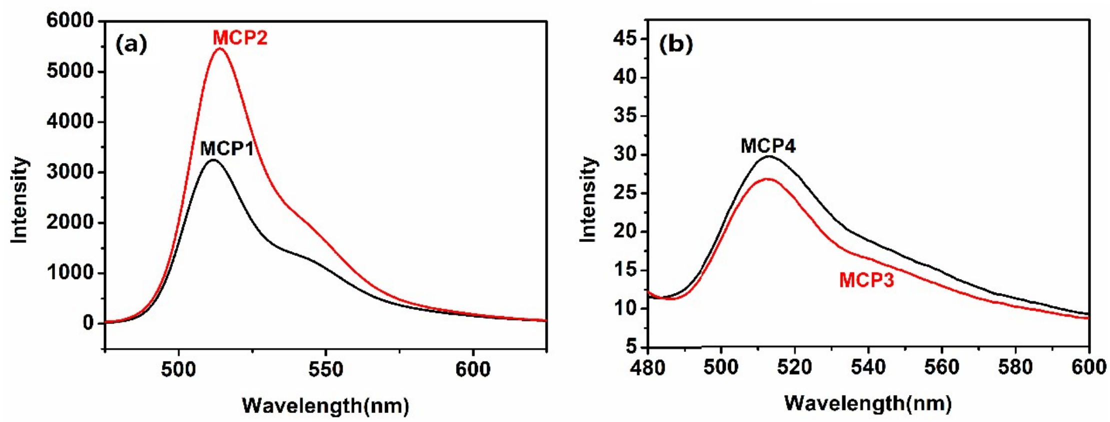


**Figure S11.** Fluorescence emission spectra of macromolecular probes (1 μM) in EtOH/$H_2O$ (1:1, rt) (a) **MCP1** and **MCP2** (λex = 440 nm), (b) **MCP3** and **MCP4** (λex = 440 nm).

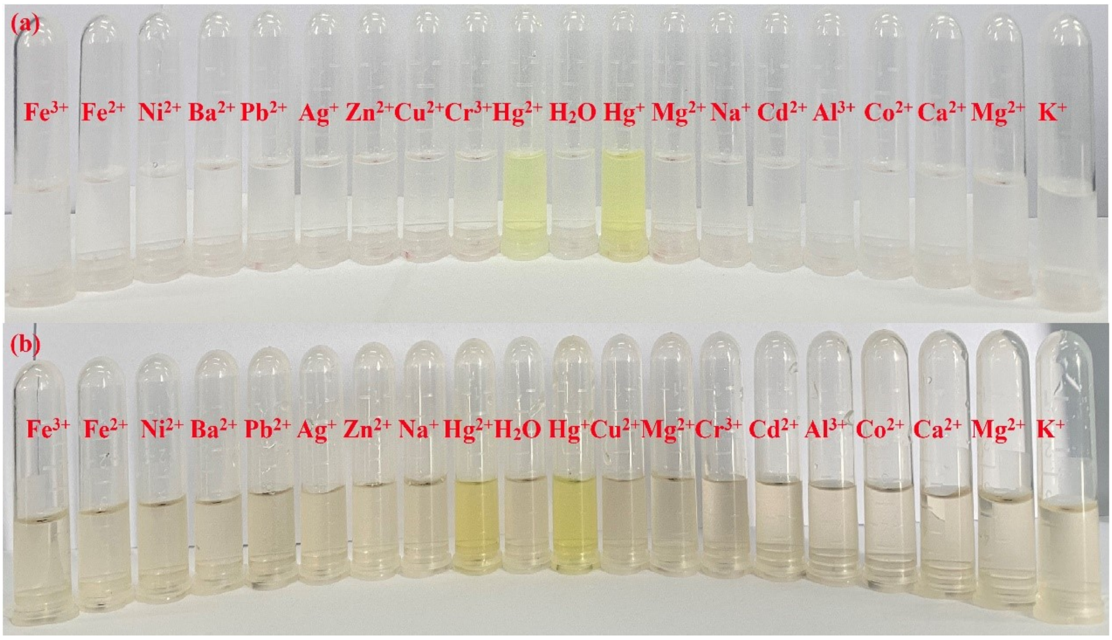


**Figure S12.** (a) photograph of **MCP3** with heavy metal ion in water under natural light. (b) photograph of **MCP4** with heavy metal ion in water under natural light.

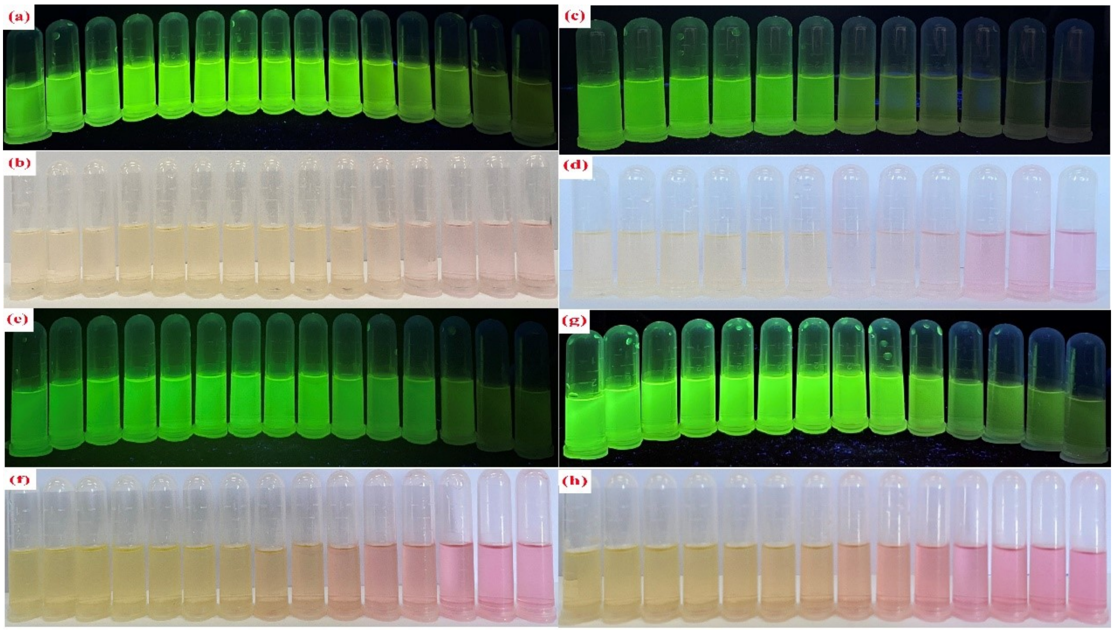


**Figure S13.** (a) photograph of **MCP1** with different concentrations of $Hg^{+}$ in EtOH/$H_2O$ under UV light. (b) photograph of **MCP1** with different concentrations of $Hg^{+}$ in EtOH/$H_2O$ under natural light. (c) photograph of **MCP1** with different concentrations of $Hg^{2+}$ in EtOH/$H_2O$ under UV light. (d) photograph of **MCP1** with different concentrations of $Hg^{2+}$ in EtOH/$H_2O$ under natural light. (e) photograph of **MCP2** with different concentrations of $Hg^{+}$ in EtOH/$H_2O$ under UV light. (f) photograph of **MCP2** with different concentrations of $Hg^{+}$ in EtOH/$H_2O$ under natural light. (g) photograph of **MCP2** with different concentrations of $Hg^{2+}$ in EtOH/$H_2O$ under UV light. (h) photograph of **MCP2** with different concentrations of $Hg^{2+}$ in EtOH/$H_2O$ under natural light.

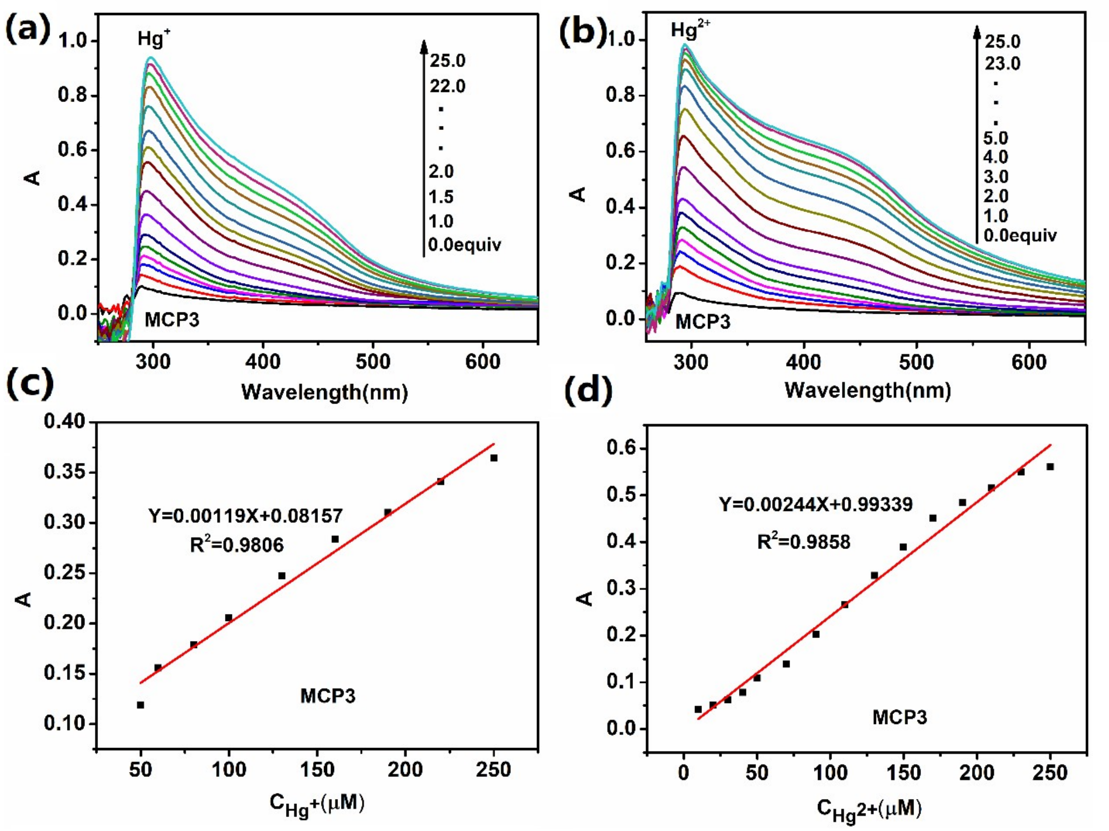


**Figure S14.** (a) Concentration effect of **MCP3** on $Hg^{+}$. (b) Concentration effect of **MCP3** on $Hg^{2+}$. (c) Concentration-dependent fluorescence signaling of a $Hg^{+}$ by **MCP3**, and (d) $Hg^{2+}$ by **MCP3**

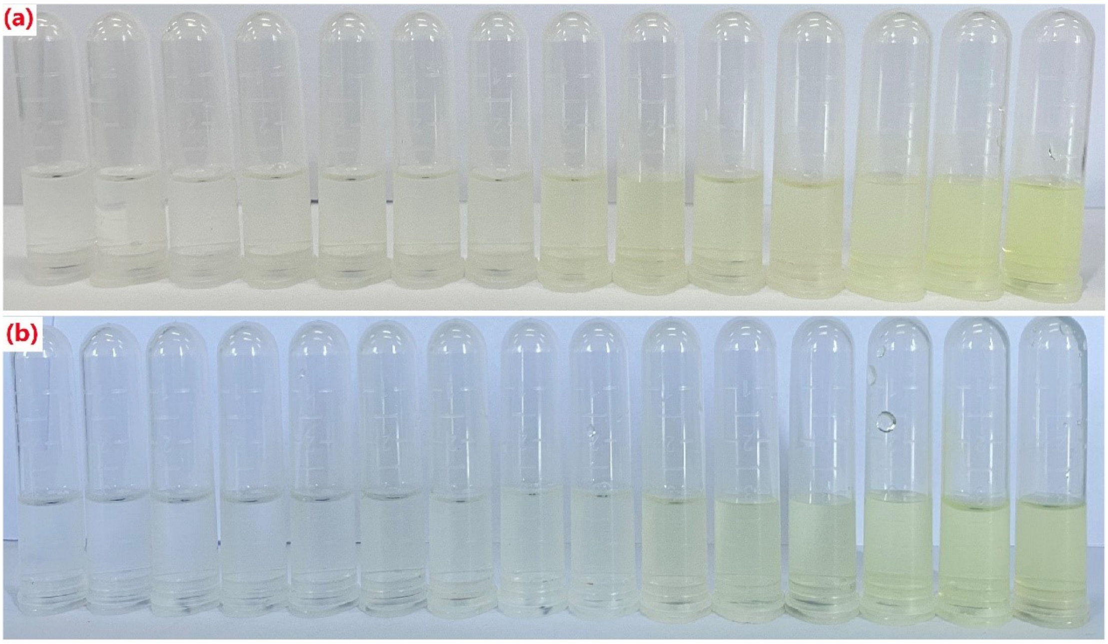


**Figure S15.** (a) photograph of **MCP3** with different concentrations of $Hg^{+}$ in water under natural light. (b) photograph of **MCP3** with different concentrations of $Hg^{2+}$ in water under natural light.

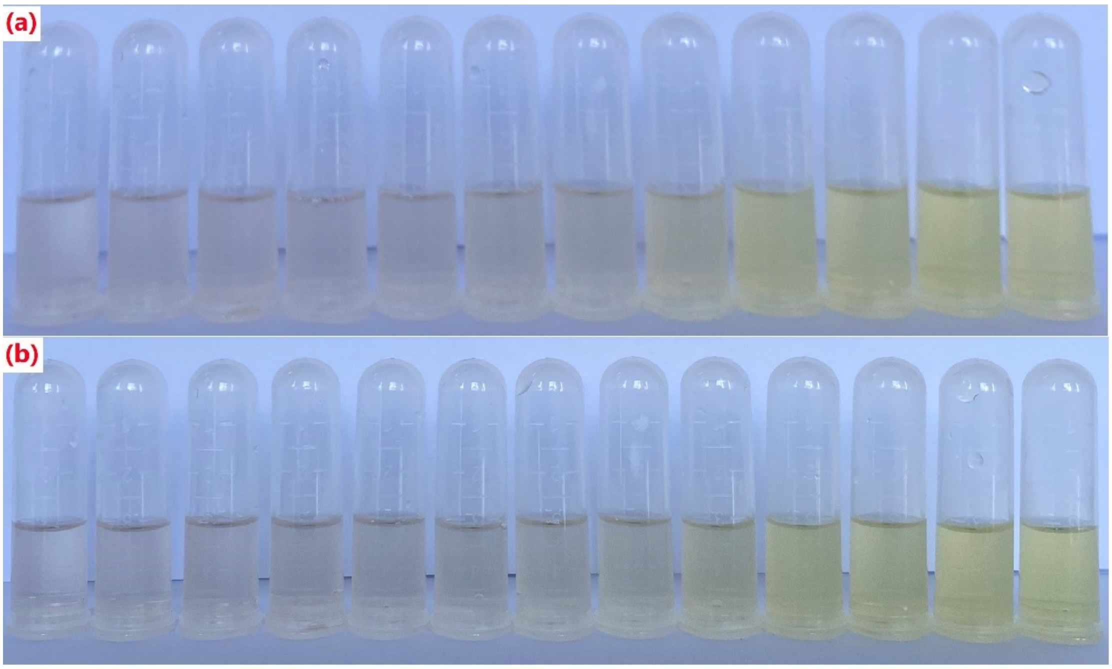


**Figure S16.** (a) photograph of **MCP4** with different concentrations of $Hg^{+}$ in water under natural light. (b) photograph of **MCP4** with different concentrations of $Hg^{2+}$ in water under natural light.

Table S1. Comparison of the basic properties of the reported probe and the probe synthesized in this article

| **Sensor** | **Selectivity** | **LOD** | **Analytical applications** | **Reference** |
|---|---|---|---|---|
| 1-CN | Good ($Hg^{2+}$) | 0.8μM | Cell image | [1] |
| 9AnPD | Effective ($Hg^{2+}$) | 5μM | -- | [2] |
| BAN | Remarkable ($Hg^{2+}$) | 0.00173 μM | Living HeLa cells | [3] |
| probe 1 | Sensitive ($Hg^{2+}$) | 0.2μM | Living cells | [4] |
| L | High ($Hg^{2+}$) | 1.1μM | Living cell imaging | [5] |
| PTS | Sensitive ($Hg^{2+}$) | 0.23μM | -- | [6] |
| RFP3 | Excellent ($Hg^{2+}$/$Cu^{2+}$) | 0.012μM | HL-7702 cells | [7] |
| P-3 | High ($Hg^{2+}$) | 4.8μM | -- | [8] |
| MCP2 | Sensitive ($Hg^{2+}$/$Hg^{+}$) | 0.32/0.42μM | Lake water | This work |

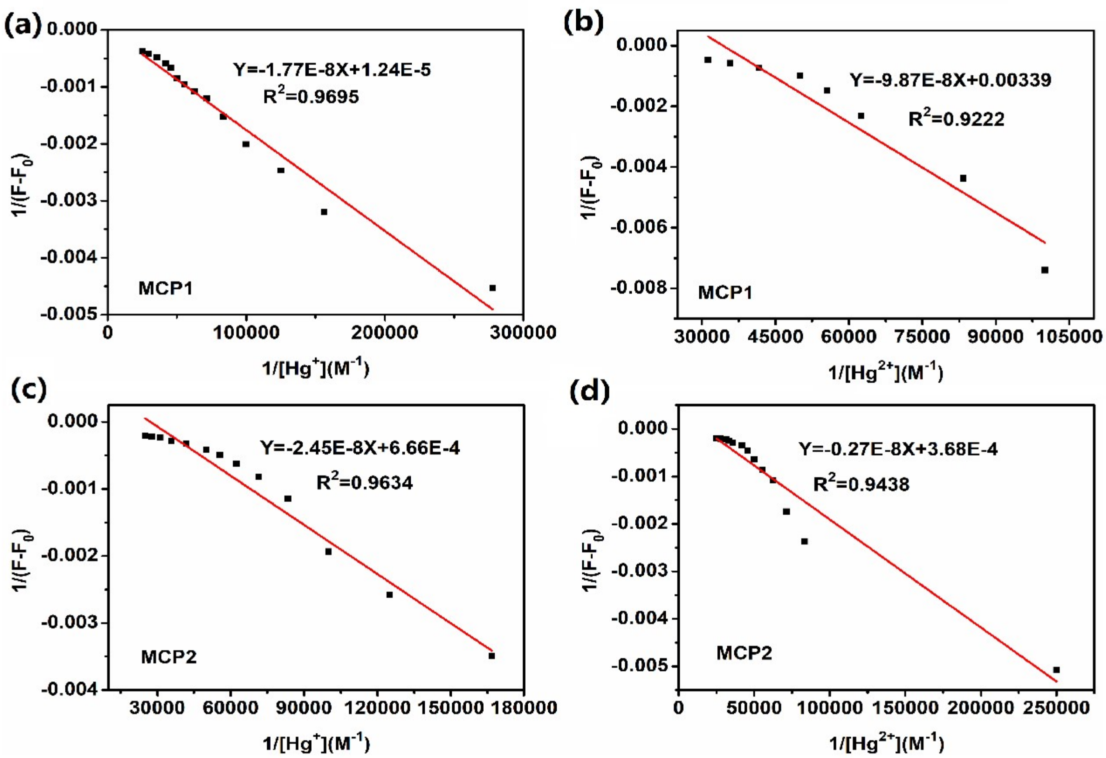


**Figure S17.** Benesi–Hilderbrand plot of (a) **MCP1**+$Hg^{+}$, (b) **MCP1**+$Hg^{2+}$, (c) **MCP2**+$Hg^{+}$, and (d) **MCP2**+$Hg^{2+}$

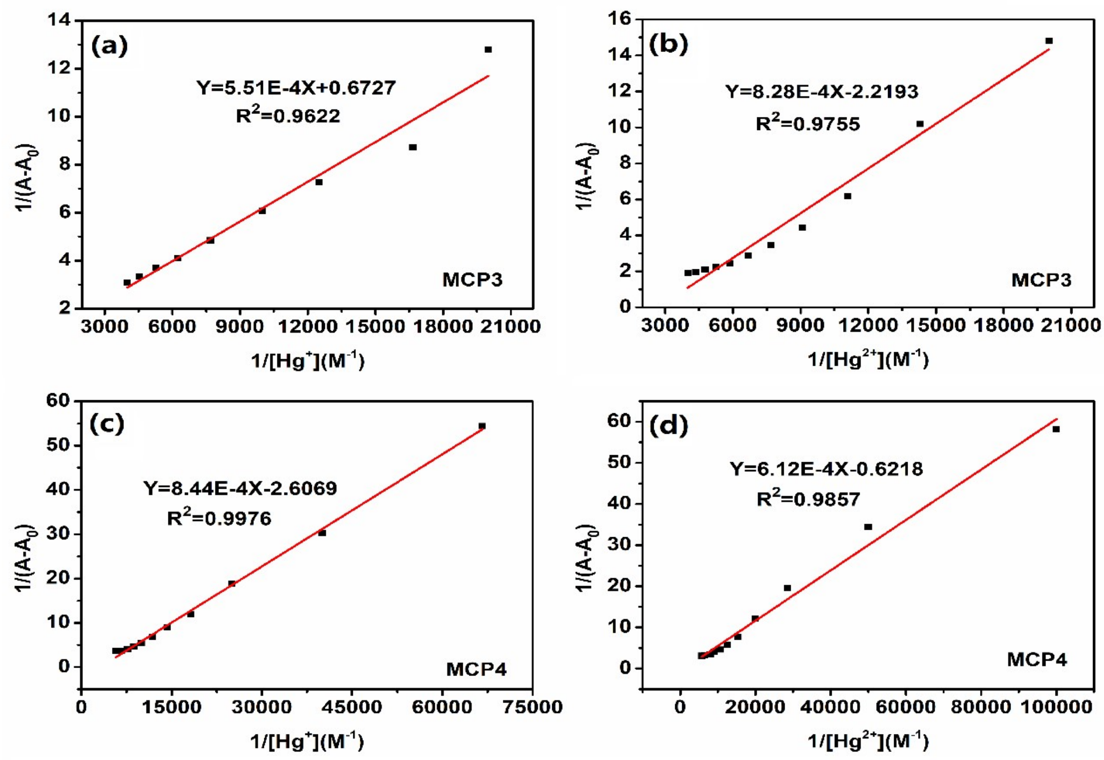


**Figure S18.** Benesi–Hilderbrand plot of (a) **MCP3**+$Hg^{+}$, (b) **MCP3**+$Hg^{2+}$, (c)

**MCP4**+$Hg^{+}$, and (d) **MCP4**+$Hg^{2+}$

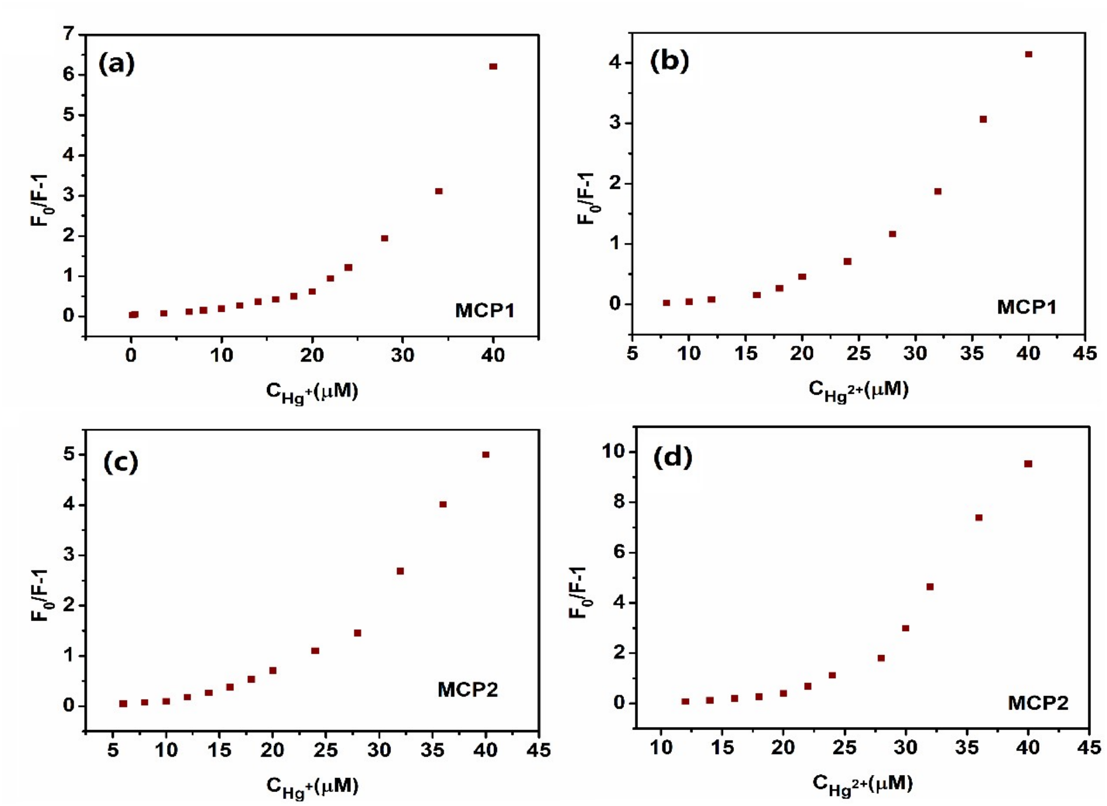


**Figure S19.** The fluorescence intensity of the polymer solution changes with the concentration of $Hg^{2+}$/$Hg^{+}$ (a) **MCP1**+$Hg^{+}$(1μM, pH = 7.0, rt); (b)**MCP1**+$Hg^{2+}$ (1μM, pH = 7.0, rt); (c)**MCP2**+$Hg^{+}$ (1μM, pH = 7.0, rt); (d)**MCP2**+$Hg^{2+}$ (1μM, pH = 7.0, rt)

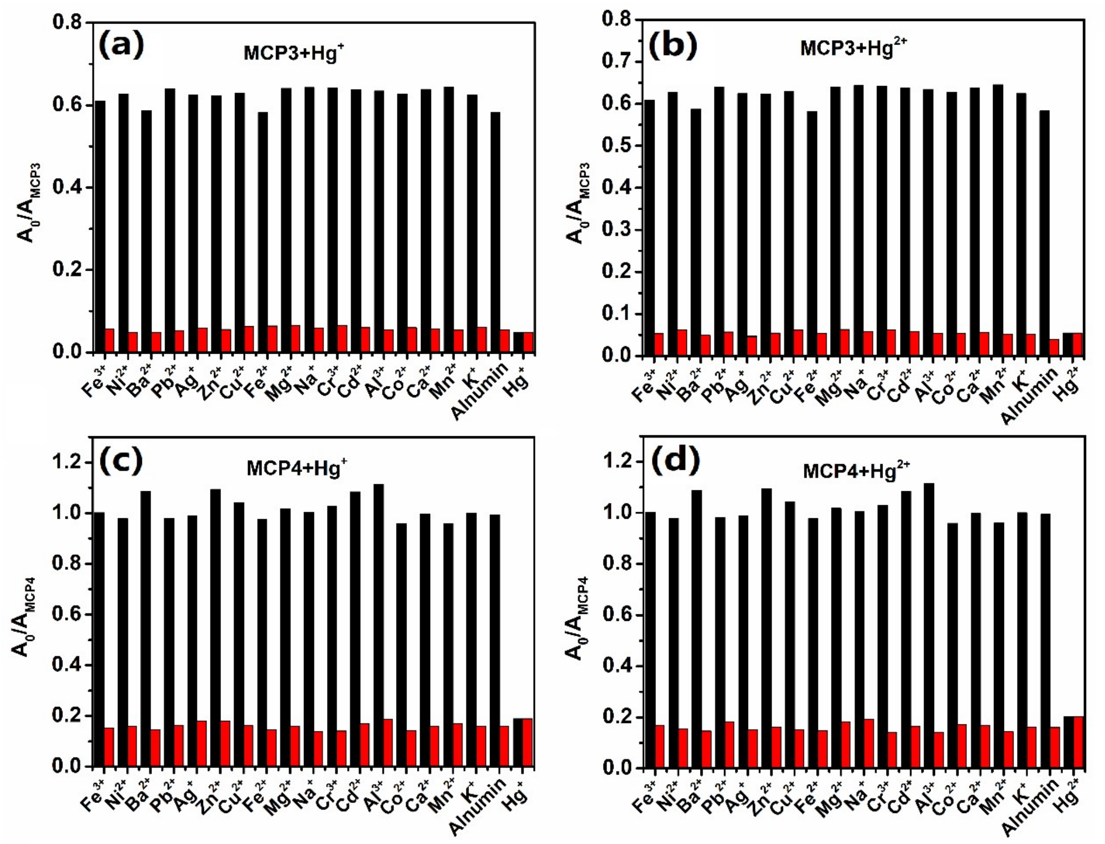


**Figure S20.** Absorbance of probes (10μM) with other metal ions (100 μM) and albumin (3.6 mg/mL) in aqueous solution. The black bars represent the addition of different ions to the solution of correspond sensor. The red bars represent the subsequent addition of $Hg^{2+}$/$Hg^{+}$ the solution.

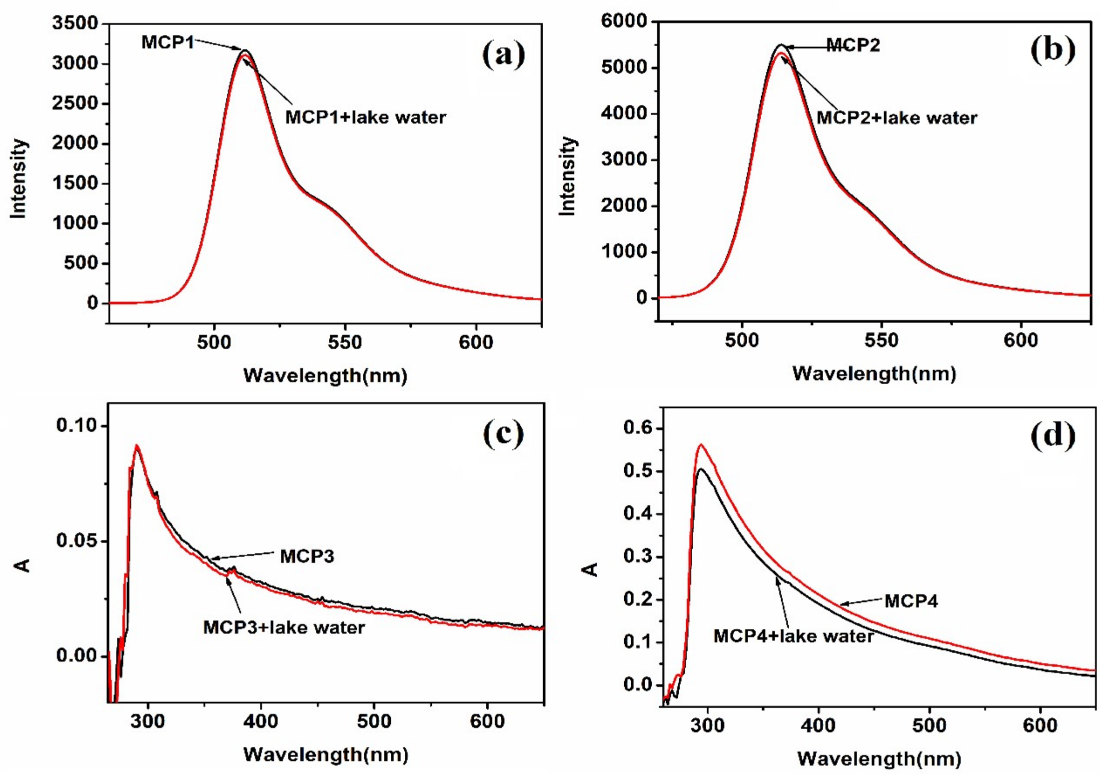


**Figure S21.** The fluorescence emission spectrum of sensor in EtOH/$H_2O$ and EtOH/natural lake water. (a) **MCP1**, (b) **MCP2**. UV absorption spectra of sensor in water and natural lake water. (c) **MCP3**, (d) **MCP4**

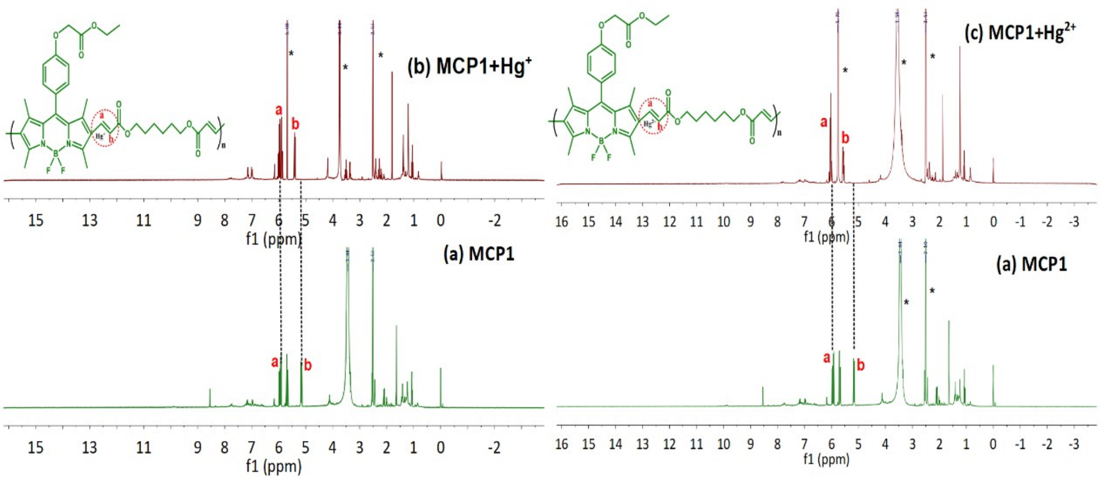


**Figure S22.** (a) $^1$H NMR of **MCP1** in DMSO-d6, (b) $^1$H NMR of **MCP1** and equimolar amount of $Hg^+$ in DMSO-d6. (c) $^1$H NMR of **MCP1** and equimolar amount of $Hg^{2+}$ in DMSO-d6.

## References

[1] J. Ding, H. Li, C. Wang, J. Yang, Y. Xie, Q. Peng, Q. Li, Z. Li, "Turn-On" Fluorescent Probe for Mercury(II): High Selectivity and Sensitivity and New Design Approach by the Adjustment of the pi-Bridge, ACS Appl Mater Interfaces 7(21) (2015) 11369-76.http://dx.doi.org/10.1021/acsami.5b01800

[2] Y. Jia, Y. Pan, H. Wang, R. Chen, H. Wang, X. Cheng, Highly selective and sensitive polymers with fluorescent side groups for the detection of Hg 2+ ion, Materials Chemistry and Physics 196 (2017) 262-269.http://dx.doi.org/10.1016/j.matchemphys.2017.05.001

[3] H. Xiao, J. Li, K. Wu, G. Yin, Y. Quan, R. Wang, A turn-on BODIPY-based fluorescent probe for Hg(II) and its biological applications, Sensors and Actuators B: Chemical 213 (2015) 343-350.http://dx.doi.org/10.1016/j.snb.2015.02.105

[4] Z. Zhu, H. Ding, Y. Wang, C. Fan, Y. Tu, G. Liu, S. Pu, A ratiometric and colorimetric fluorescent probe for the detection of mercury ion based on rhodamine and quinoline–benzothiazole conjugated dyad, Journal of Photochemistry and Photobiology A: Chemistry 400 (2020).http://dx.doi.org/10.1016/j.jphotochem.2020.112657

[5] W. Feng, Q. Xia, H. Zhou, Y. Ni, L. Wang, S. Jing, L. Li, W. Ji, A fluorescent probe based upon anthrancene-dopamine thioether for imaging Hg(2+) ions in living cells, Talanta 167 (2017) 681-687.http://dx.doi.org/10.1016/j.talanta.2017.03.012

[6] Y. Shan, W. Yao, Z. Liang, L. Zhu, S. Yang, Z. Ruan, Reaction-based AIEE-active conjugated polymer as fluorescent turn on probe for mercury ions with good sensing performance, Dyes and Pigments 156 (2018) 1-7.http://dx.doi.org/10.1016/j.dyepig.2018.03.060

[7] M. Wang, F. Yan, Y. Zou, L. Chen, N. Yang, X. Zhou, Recognition of Cu2+ and Hg2+ in physiological conditions by a new rhodamine based dual channel fluorescent probe, Sensors and Actuators B: Chemical 192 (2014) 512-521.http://dx.doi.org/10.1016/j.snb.2013.11.031

[8] Y. Lei, F. Ma, Y. Tian, Q. Niu, H. Mi, I. Nurulla, W. Shi, Fluorene-based conjugated polymer with tethered thymines: click postpolymerization synthesis and optical response to mercury(II), Journal of Applied Polymer Science 129(4) (2013) 1763-1772.http://dx.doi.org/10.1002/app.38817